nature climate change

LETTERS

PUBLISHED ONLINE: 7 DECEMBER 2015 | DOI: 10.1038/NCLIMATE2878

Foliar temperature acclimation reduces simulated carbon sensitivity to climate

Nicholas G. Smith[1]*, Sergey L. Malyshev[2], Elena Shevliakova[2], Jens Kattge[3,4] and Jeffrey S. Dukes[1,5]

Plant photosynthesis and respiration are the largest carbon fluxes between the terrestrial biosphere and the atmosphere[1], and their parameterizations represent large sources of uncertainty in projections of land carbon uptake in Earth system models[2,3] (ESMs). The incorporation of temperature acclimation of photosynthesis and foliar respiration, commonly observed processes, into ESMs has been proposed as a way to reduce this uncertainty[2]. Here we show that, across 15 flux tower sites spanning multiple biomes at various locations worldwide (10° S–67° N), acclimation parameterizations[4,5] improve a model's ability to reproduce observed net ecosystem exchange of CO_2. This improvement is most notable in tropical biomes, where photosynthetic acclimation increased model performance by 36%. The consequences of acclimation for simulated terrestrial carbon uptake depend on the process, region and time period evaluated. Globally, including acclimation has a net effect of increasing carbon assimilation and storage, an effect that diminishes with time, but persists well into the future. Our results suggest that land models omitting foliar temperature acclimation are likely to overestimate the temperature sensitivity of terrestrial carbon exchange, thus biasing projections of future carbon storage and estimates of policy indicators such as the transient climate response to cumulative carbon emissions[1].

The terrestrial components of Earth system models (ESMs) simulate a variety of physiological and ecological processes to project carbon storage and terrestrial feedbacks to climate. These processes strongly affect simulated land–atmosphere interactions[6], with consequences for historical and future climate projections that rival or exceed many atmospheric processes[2,7]. Although the temperature sensitivity of the terrestrial carbon cycle has been considered a fundamental characteristic of Earth's carbon cycle, rigorously analysed in many studies and assessments (for example, ref. 1), some relevant, observed and well-characterized processes are still omitted from many ESMs (ref. 6), including those used in the Coupled Model Intercomparison Project, phase 5 (CMIP5; ref. 8). Examples of such processes are temperature acclimation of photosynthesis and leaf respiration, the gradual adjustment of the instantaneous temperature response of these two key processes of the terrestrial carbon cycle as a result of longer-term changes in growth temperature[9–11].

Previous studies have found that the uncertainty in ESMs' projection of future carbon uptake is strongly related to the parametric uncertainty in the temperature response formulations for leaf photosynthesis and respiration[2,3]. For example, results of one set of simulations suggested that the primary parameter driving uncertainty in terrestrial carbon–climate feedbacks was the optimum temperature for photosynthesis (T_{opt}), which was not allowed to change (that is, acclimate) in the study[2]. Consequently, it has been proposed that temperature acclimation might improve model functioning[2] and, by decreasing the temperature sensitivity of acclimated processes, increase simulated carbon uptake on land[12,13]. These results, in part, have led to the inclusion of temperature acclimation of photosynthesis and/or leaf respiration in some global-scale land models[14].

Here, we explore the influence of state-of-the-art, empirically derived acclimation parameterizations of both photosynthesis and foliar respiration[4,5] on model performance across multiple biomes and examine how these parameterizations will affect simulated leaf carbon exchange processes and simulated terrestrial carbon storage, from pre-industrial periods to 2100. We reasoned that, because temperature acclimation of photosynthesis and foliar respiration is widely observed (as reviewed in refs 11,14,15; see also citations in the Supplementary Methods), acclimation parameterizations would enhance a model's ability to reproduce observed carbon exchange rates. Additionally, we expected that acclimation would increase the net carbon assimilation of leaves by decreasing the sensitivity of leaf carbon exchange to temperature, resulting in high rates of carbon uptake across a wider range of temperatures, ultimately leading to increases in terrestrial carbon storage.

Most terrestrial ecosystem models and CMIP5-class ESMs simulate photosynthesis as the minimum of two rate-limiting steps involved in the Calvin cycle: Rubisco carboxylation (V_c) and ribulose-1,5,-bisphosphate regeneration (J), processes that are scaled by their maximum rates (V_{cmax} and J_{max}, respectively)[16]. V_{cmax} and J_{max} are commonly defined by a basal rate (that is, the rate at a standardized temperature) that is modified by a peaked Arrhenius-type temperature function[14]. No mechanistic algorithm has been developed for leaf carbon release (that is, respiration)[17]. Instead, dark respiration (R_d) is commonly simulated as a function of a basal rate that is typically linked to the photosynthetic rate, and an exponential temperature function[14].

Temperature acclimation parameterizations have been developed for V_{cmax}, J_{max} and R_d. At present, the most frequently used, robust, widely cited, and thus state-of-the-art, acclimation parameterizations are those defined by Kattge and Knorr[4] for V_{cmax} and J_{max} and Atkin *et al.*[5] for R_d. The Kattge and Knorr[4] formulation for photosynthetic acclimation was derived using empirical data from 36 different species and allows for the optimum temperature of the instantaneous temperature response of J_{max}

[1]Department of Biological Sciences, Purdue University, West Lafayette, Indiana 47907, USA. [2]Princeton University & Geophysical Fluid Dynamics Laboratory Cooperative Institute for Climate Studies, Princeton, New Jersey 08540, USA. [3]Max Planck Institute for Biogeochemistry, Jena 07745, Germany. [4]German Centre for Integrative Biodiversity Research Halle-Jena-Leipzig, Leipzig 04103, Germany. [5]Department of Forestry and Natural Resources, Purdue University, West Lafayette, Indiana 47907, USA. *e-mail: ngsmith@purdue.edu

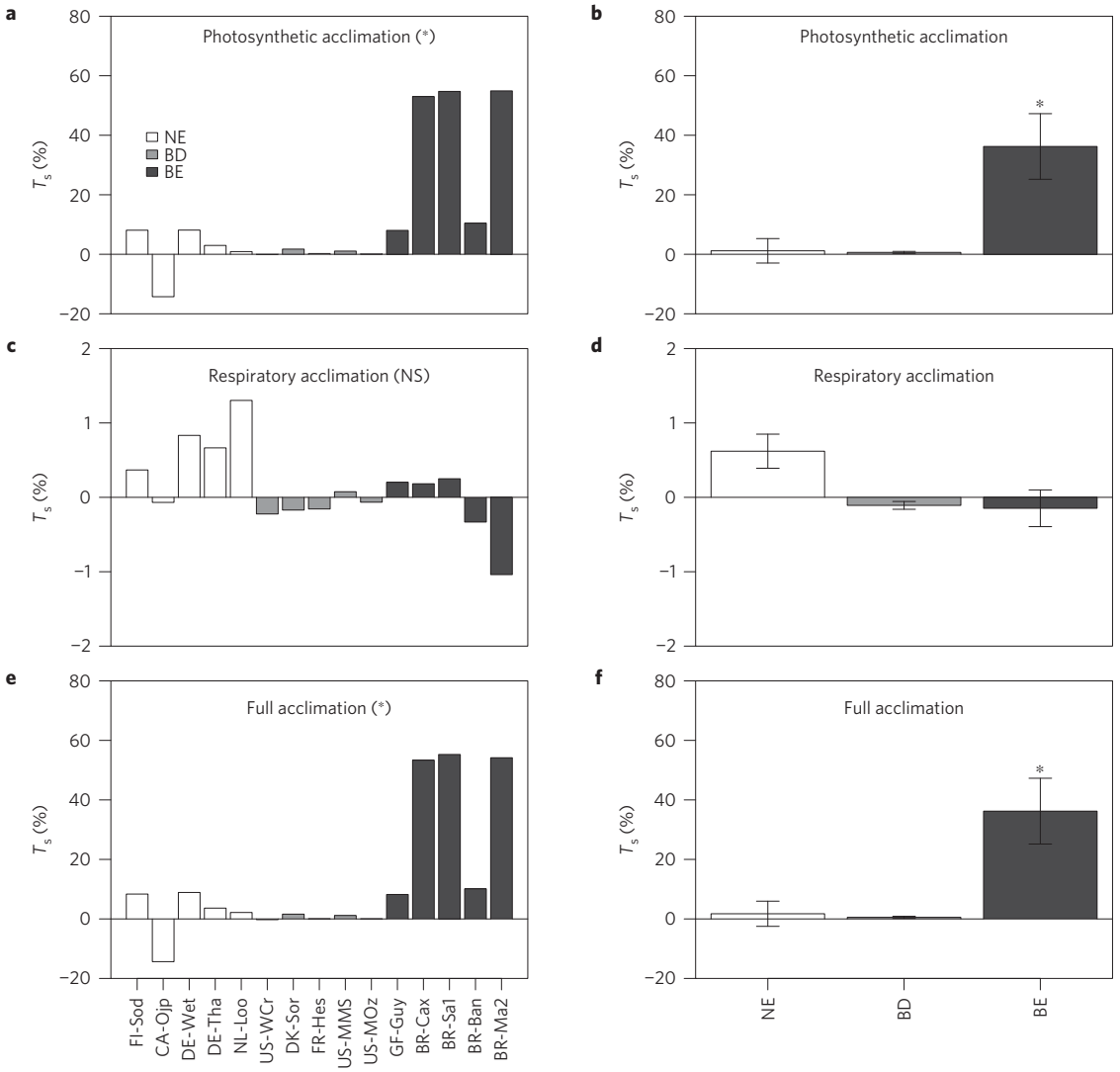

Figure 1 | Model improvement by acclimation. a–f, Percentage change in Taylor scores (T_s) for net ecosystem exchange (NEE) in simulations with photosynthetic (**a**,**b**), respiratory (**c**,**d**), and both photosynthetic and respiratory acclimation (**e**,**f**) compared with simulations without any temperature acclimation. The left panels show results from each flux tower site and asterisks in the panel title indicate significant results across all sites (see Supplementary Table 1 for forest type abbreviations) (NS, not significant). The right three panels show results averaged across forest types with asterisks above bars indicating significant results within forest types. Significant results were determined using Bayesian *t*-tests (see Methods). Error bars are the standard error of the mean.

and V_{cmax} as well as the ratio of J_{max} to V_{cmax} at 25 °C (J/V) to shift with the mean air temperature over the previous 30 days (see Methods). The Atkin *et al.*[5] parameterization for temperature acclimation of foliar respiration was derived using empirical data from 19 species and includes a correction factor that allows the basal rate of respiration to shift with the mean air temperature over the previous 10 days (see Methods). Although based on limited data sets, these parameterizations are state-of-the-art and implemented in global-scale land models (for example, ref. 3). Nevertheless, the influence of these parameterizations on simulated carbon has been evaluated in only a few cases (for example, refs 5,6; see additional references in the Supplementary Methods) and their influence on model performance has not yet been examined.

To explore the influence of foliar temperature acclimation parameterizations on model performance, we used Land Model version 3 (LM3; ref. 18), a process-based land model that is the terrestrial component of the National Oceanic and Atmospheric Administration/Geophysical Fluid Dynamics Laboratory (NOAA/GFDL) ESMs, driven by high-frequency (three-hourly) observed climate forcing[19] to simulate historical net ecosystem exchange (NEE) rates in 15 different grid cells encompassing 15 observational eddy-covariance flux tower sites. The sites represent three types of forest (five sites in each type): broadleaf deciduous (BD), needleleaf evergreen (NE), and broadleaf evergreen (BE; Supplementary Table 1 and Supplementary Fig. 1). Note that BD and BE sites were located exclusively in temperate and tropical climates, respectively, whereas NE sites were located in temperate and boreal climates. We compared the simulated fluxes to observations at each site using Taylor scores, which track both the absolute values as well as the variation in these values between modelled and observed responses[20]. We compared Taylor scores from simulations without acclimation to simulations with either photosynthetic acclimation, respiratory acclimation, or both, using Bayesian paired *t*-tests[21] (see Methods).

We found that, when analysed across all forest types or within each forest type separately, acclimation improved or had no significant effect on model performance. When both photosynthetic

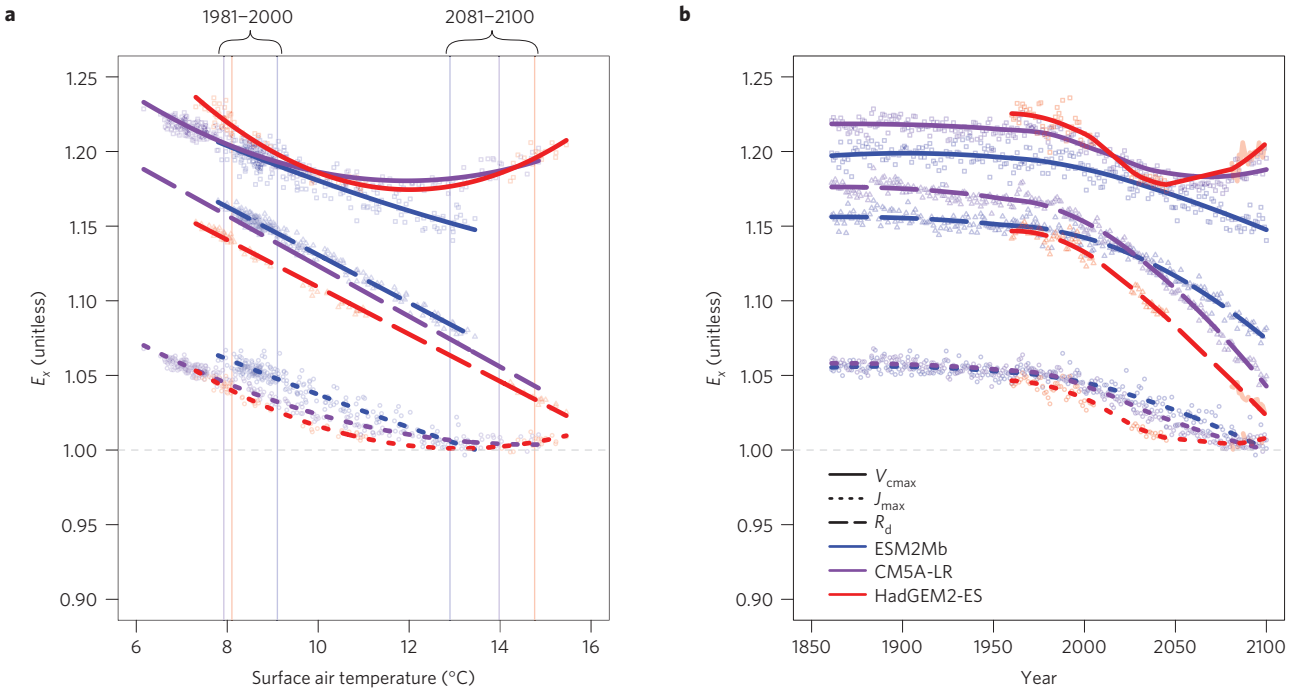

Figure 2 | Global influence of acclimation on photosynthesis and foliar respiration. a,**b**, Annual, globally averaged effect of acclimation (E_x; see Methods) for V_{cmax} (squares), J_{max} (circles) and R_d (triangles) as a function of mean global land surface air temperature (**a**; SAT) and time (**b**) from 1861 to 2100. Data were generated using output from three different ESM simulations forced by the RCP 8.5 scenario. Trendlines in **a** show parabolic (V_{cmax} and J_{max}) and linear (R_d) model fit to the data. Smoothed lines in **b** were created using a loess function with an alpha value of 0.75. The horizontal dashed grey line represents $E_x = 1$. The vertical lines in **a** show the mean global land surface air temperature for the three models over two time periods.

and respiratory temperature acclimation were included, model simulations of observed NEE significantly improved Taylor scores by 12.8% (see Supplementary Table 2 for full Bayesian paired t-test results). Improvements from photosynthetic acclimation strongly outweighed those from respiratory acclimation, where Taylor scores did not change by more than 2% at any site (Fig. 1). The influence of acclimation differed among forest types. Photosynthetic acclimation significantly improved model performance at the tropical (that is, BE) sites, but had variable, nonsignificant effects at the BD and NE sites (Fig. 1 and Supplementary Table 2). Respiratory acclimation had a more consistent, but nonsignificant, positive effect at needleleaf compared with broadleaf sites. As respiratory acclimation had little effect on Taylor scores, results from simulations with both types of acclimation mirrored the results from simulations that included only photosynthetic acclimation.

To explore the implications of these acclimation parameterizations[4,5] for projections of the carbon cycle at the global scale, we calculated the effect of acclimation (E_x) for each process (that is, E_v, E_j, and E_r for V_{cmax}, J_{max}, and R_d, respectively), defined as the ratio of the acclimated rate to the unacclimated rate of each process. Unacclimated rates were calculated using mean values for ΔS_v, ΔS_j and J/V from Kattge and Knorr[4] and without the correction factor for R_d. We computed E_v, E_j, and E_r for each land grid cell using high-frequency (three-hourly) climate and ecological output from 1861–2100 from three historical and representative concentration pathway (RCP) 8.5 forcing scenario[22] simulations from the CMIP5 (ref. 8). We used available high-frequency output from three ESMs: NOAA/GFDL ESM2M (refs 23,24), Institut Pierre Simon Laplace (IPSL) CM5A-LR (ref. 25), and Met Office Hadley Center (MOHC) HadGEM2-ES (ref. 26). The values were linearly weighted by gross primary productivity for V_{cmax} and J_{max} and total plant respiration for R_d in computing global land annual averages. This allowed more productive regions and seasons to give stronger weight to the results (see Methods).

We found that, when averaged globally under past, current and future climates (that is, 1861–2100), acclimated V_{cmax}, J_{max} and R_d were consistently higher than non-acclimated rates (Fig. 2), implying that temperature acclimation increases simulated rates of these processes. Increases in photosynthetic carbon assimilation and respiratory carbon loss should have counteracting effects on net leaf carbon assimilation. This respiratory response was not consistent with our hypothesis. However, the global effect on R_d decreases linearly with increasing global-mean temperature (that is, ratio moves closer to 1; Fig. 2), implying that respiratory acclimation could promote carbon uptake by decreasing R_d under future, warmer conditions. This effect resulted from using a basal rate acclimation formulation, which acts to increase process rates below the temperature used for standardization and decrease them above this temperature as compared with unacclimated rates[5]. Interestingly, the nonlinear shapes of the E_v and E_j responses to surface air temperature (Fig. 2) suggest that acclimation will continue to amplify simulated photosynthetic rates under future, warmer conditions at the global scale. Specifically, this nonlinear shape suggests that acclimation will have the greatest positive effect on V_{cmax} and J_{max} at cold and warm extremes. However, the shape of E_j also suggests that acclimation may decrease J_{max} at some relatively high global temperatures.

We examined how these results varied geographically using forcing from a single ESM (that is, NOAA/GFDL ESM2M) while excluding points where vegetation was either absent or dormant (that is, leaf area index of zero) and reducing the weight of points at extremely low and high temperatures under which productivity would not be supported (see Methods). We found that acclimation formulations increased V_{cmax} and decreased R_d and J_{max} throughout the entire time period in low-latitude, tropical regions and decreased R_d in more regions in the future as temperatures warmed, as compared with the formulations without acclimation. In contrast, acclimation increased all three simulated processes

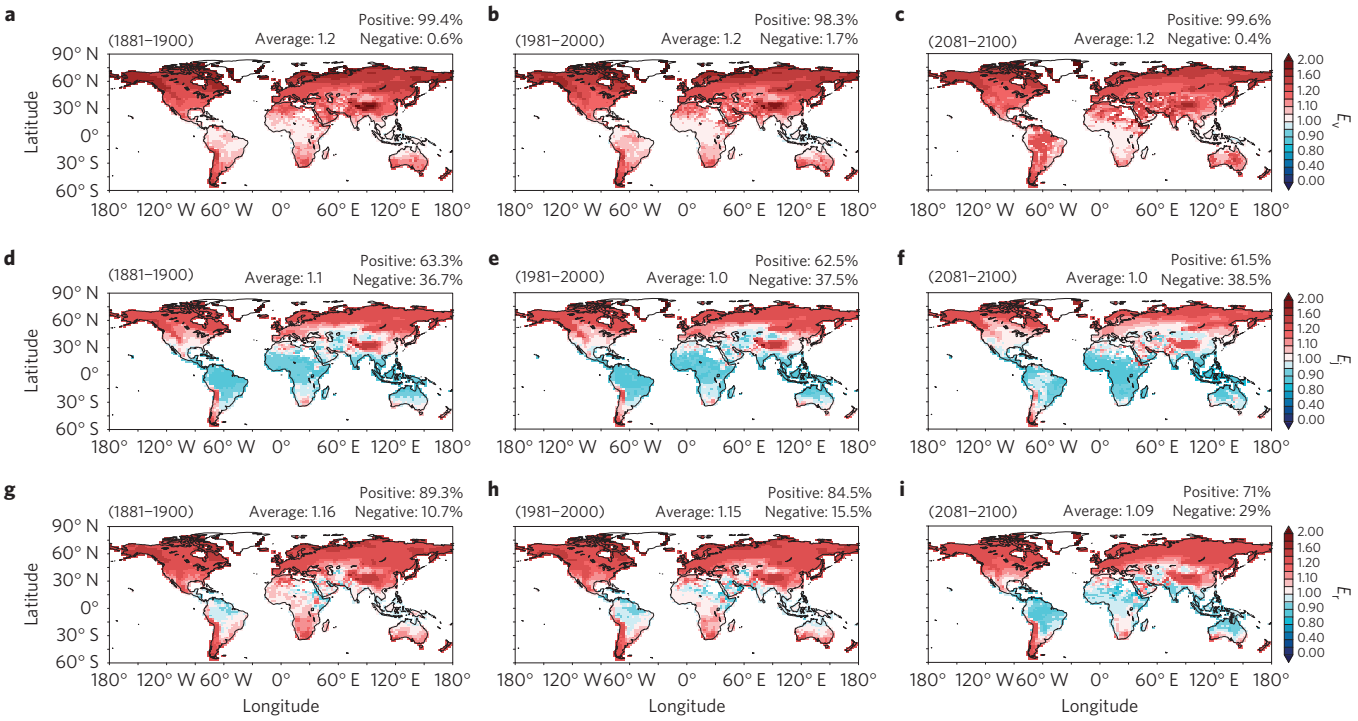

Figure 3 | Global maps of the influence of acclimation on each process at the ends of the nineteenth, twentieth and twenty-first centuries. a–i, The average effect of acclimation (see Methods) for V_{cmax} (E_v; **a**–**c**), J_{max} (E_j; **d**–**f**), and R_d (E_r; **g**–**i**) from 1881–1900 (**a**,**d**,**g**), 1981–2000 (**b**,**e**,**h**), and 2081–2100 (**c**,**f**,**i**). Data were generated using output from GFDL ESM2Mb ESM simulation forced by the RCP 8.5 scenario. The global average value and the percentage of grid cells showing positive (>1) or negative (<1) influence of acclimation are shown above each panel.

in cooler, extra-tropical regions (Fig. 3), thus amplifying both carbon assimilation through photosynthesis and loss through foliar respiration. The decrease in J_{max} with acclimation in tropical regions reflects the sensitivity of processes involved in light capture and electron transport to high temperature[27] and follows from the nonlinear curve observed in the global analysis (Fig. 2). This effect is the result of a decrease in the J/V ratio as growth temperatures increase[4] (see Methods), which causes a decrease in the acclimated compared with unacclimated rate of J_{max}. Notably, this decrease is lessened under future, warmer conditions as shifts in the optimum temperature for J_{max} increase the acclimated above the unacclimated rates (for example, Fig. 3e,f). In summary, the net effect of acclimation on simulated carbon uptake will depend in part on the process, time period and region evaluated. Additionally, the net result is likely to differ between models (see additional discussion in Supplementary Methods).

To illustrate the effect of foliar temperature acclimation on future global carbon dynamics, we applied photosynthetic and respiratory acclimation parameterizations to the terrestrial component LM3 of the NOAA/GFDL ESM2M and compared simulated vegetation carbon during 1861–2099 to the original LM3 simulations with the same climate forcing (see Methods). We found that foliar temperature acclimation increased simulated global vegetation carbon from 1860 to 2100 compared with the simulation without acclimation (Fig. 4). As our process-scaling analysis indicated (see above), the magnitude of simulated acclimation response varies spatially and temporally. For example, the acclimation effect was strongest in the coldest regions (Supplementary Fig. 2) owing to beneficial effects of photosynthetic acclimation (see Supplementary Figs 3 and 4) and despite a reduction due to respiration acclimation (Supplementary Fig. 5), which had little effect on future simulations in general. Also, acclimation decreased vegetation carbon in warm regions (Supplementary Fig. 2). The difference between global vegetation carbon in acclimated and non-acclimated simulation decreased over time as global temperatures warmed (Fig. 4, see also Supplementary Methods). The attenuation of the acclimation effect was probably the result of a decrease in the J/V ratio under increasing growth temperatures reducing acclimated J_{max} rates compared with unacclimated rates (Figs 2 and 3). This is an understudied phenomenon, particularly in tropical plants, that deserves further evaluation.

Many empirical studies have documented leaf-level temperature acclimation[11,14,15] (see additional references in the Supplementary Methods), but relatively few have collected the type of data necessary to constrain and parameterize acclimation functions[14]. Although we used the most robust acclimation functions available[4,5], they were derived using only a small number of (primarily temperate) species. Plant species and/or plant functional types might differ in their acclimation capacity, as evolutionary pressures to adjust to changes in seasonal temperatures may vary among regions[9,10], but tests of this hypothesis are scarce and show conflicting results[11,15]. Our model–data comparison indicates that species differences are likely to exist (Fig. 1). In addition, some plant species might be expected to adapt to warmer temperatures in the future on multi-decadal or longer timescales not considered in the acclimation formulations evaluated here. Finally, as extreme warm temperatures are expected to be more frequent in the future[28], acclimation may dampen the effect of such warm episodes on simulated plant carbon uptake. There is still a great deal of uncertainty associated with contemporary acclimation formulations[3] and further refinement of photosynthetic and respiratory processes is needed to better constrain carbon cycle models at the global scale.

Our findings indicate that climate models that do not include temperature acclimation of foliar carbon exchange are likely to overestimate carbon sensitivity to a warming climate, which affects simulations of future terrestrial carbon storage. Incorporating foliar temperature acclimation processes will reduce uncertainty in future

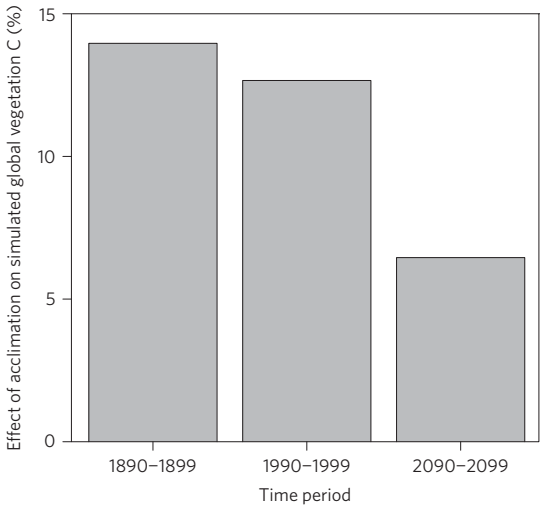

Figure 4 | Effect of acclimation on global simulated vegetation carbon in LM3. The change (%) in simulated global vegetation carbon (C) from 1890–1899, 1990–1999 and 2090–2099 under the RCP 8.5 forcing scenario with full photosynthetic and foliar respiratory temperature acclimation as compared with a similar simulation without any temperature acclimation.

projections of carbon storage sensitivity to warming—the key component of policy indicators such as the transient climate response to cumulative carbon emissions[1].

Methods

Methods and any associated references are available in the online version of the paper.

Received 16 September 2014; accepted 8 October 2015; published online 7 December 2015

References

1. IPCC in *Climate Change 2013: The Physical Science Basis* (eds Stocker, T. F. *et al.*) (Cambridge Univ. Press, 2013).
2. Booth, B. B. *et al.* High sensitivity of future global warming to land carbon cycle processes. *Environ. Res. Lett.* **7,** 024002 (2012).
3. Ziehn, T., Kattge, J., Knorr, W. & Scholze, M. Improving the predictability of global CO_2 assimilation rates under climate change. *Geophys. Res. Lett.* **38,** L10404 (2011).
4. Kattge, J. & Knorr, W. Temperature acclimation in a biochemical model of photosynthesis: a reanalysis of data from 36 species. *Plant Cell Environ.* **30,** 1176–1190 (2007).
5. Atkin, O. K. *et al.* Using temperature-dependent changes in leaf scaling relationships to quantitatively account for thermal acclimation of respiration in a coupled global climate-vegetation model. *Glob. Change Biol.* **14,** 2709–2726 (2008).
6. Arneth, A., Mercado, L., Kattge, J. & Booth, B. Future challenges of representing land-processes in studies on land-atmosphere interactions. *Biogeosciences* **9,** 3587–3599 (2012).
7. Shevliakova, E. *et al.* Historical warming reduced due to enhanced land carbon uptake. *Proc. Natl Acad. Sci. USA* **110,** 16730–16735 (2013).
8. Taylor, K. E., Stouffer, R. J. & Meehl, G. A. An overview of CMIP5 and the experiment design. *Bull. Am. Meteorol. Soc.* **93,** 485–498 (2011).
9. Berry, J. & Björkman, O. Photosynthetic response and adaptation to temperature in higher plants. *Annu. Rev. Plant Physiol. Plant Mol. Biol.* **31,** 491–543 (1980).
10. Atkin, O. K., Bruhn, D., Hurry, V. M. & Tjoelker, M. G. The hot and the cold: unravelling the variable response of plant respiration to temperature. *Funct. Plant Biol.* **32,** 87–105 (2005).
11. Way, D. A. & Yamori, W. Thermal acclimation of photosynthesis: on the importance of adjusting our definitions and accounting for thermal acclimation of respiration. *Photosynth. Res.* **119,** 89–100 (2014).
12. Galbraith, D. *et al.* Multiple mechanisms of Amazonian forest biomass losses in three dynamic global vegetation models under climate change. *New Phytol.* **187,** 647–665 (2010).
13. King, A. W., Gunderson, C. A., Post, W. M., Weston, D. J. & Wullschleger, S. D. Photosynthesis in balance with respiration? Response. *Science* **313,** 917–918 (2006).
14. Smith, N. G. & Dukes, J. S. Plant respiration and photosynthesis in global-scale models: incorporating acclimation to temperature and CO_2. *Glob. Change Biol.* **19,** 45–63 (2013).
15. Slot, M. & Kitajima, K. General patterns of acclimation of leaf respiration to elevated temperatures across biomes and plant types. *Oecologia* **177,** 885–900 (2014).
16. Farquhar, G., von Caemmerer, S. & Berry, J. A biochemical model of photosynthetic CO_2 assimilation in leaves of C_3 species. *Planta* **149,** 78–90 (1980).
17. Atkin, O. K., Meir, P. & Turnbull, M. H. Improving representation of leaf respiration in large-scale predictive climate–vegetation models. *New Phytol.* **202,** 743–748 (2014).
18. Shevliakova, E. *et al.* Carbon cycling under 300 years of land use change: importance of the secondary vegetation sink. *Glob. Biogeochem. Cycles* **23,** GB2022 (2009).
19. Sheffield, J., Goteti, G. & Wood, E. F. Development of a 50-year high-resolution global dataset of meteorological forcings for land surface modeling. *J. Clim.* **19,** 3088–3111 (2006).
20. Taylor, K. E. Summarizing multiple aspects of model performance in a single diagram. *J. Geophys. Res.* **106,** 7183–7192 (2001).
21. Kruschke, J. K. Bayesian estimation supersedes the t test. *J. Exp. Psychol.* **142,** 573–603 (2013).
22. Riahi, K. *et al.* RCP 8.5—A scenario of comparatively high greenhouse gas emissions. *Climatic Change* **109,** 33–57 (2011).
23. Dunne, J. P. *et al.* GFDL's ESM2 global coupled climate–carbon Earth system models. Part I: physical formulation and baseline simulation characteristics. *J. Clim.* **25,** 6646–6665 (2012).
24. Dunne, J. P. *et al.* GFDL's ESM2 global coupled climate–carbon Earth system models. Part II: carbon system formulation and baseline simulation characteristics. *J. Clim.* **26,** 2247–2267 (2012).
25. Dufresne, J. L. *et al.* Climate change projections using the IPSL-CM5 Earth system model: from CMIP3 to CMIP5. *Clim. Dynam.* **40,** 2123–2165 (2013).
26. Collins, W. J. *et al.* Development and evaluation of an Earth-system model—HadGEM2. *Geosci. Model Dev. Discuss.* **4,** 997–1062 (2011).
27. Medlyn, B. E. *et al.* Temperature response of parameters of a biochemically based model of photosynthesis. II. A review of experimental data. *Plant Cell Environ.* **25,** 1167–1179 (2002).
28. IPCC in *Managing the Risks of Extreme Events and Disasters to Advance Climate Change Adaptation* (eds Field, C. B. *et al.*) (Cambridge Univ. Press, 2012).

Acknowledgements

This project was supported by student exchange funding for N.G.S. provided by the INTERFACE RCN (NSF DEB-0955771), a Purdue Climate Change Research Center graduate fellowship to N.G.S., and a NASA Earth and Space Science fellowship to N.G.S. (NNX13AN65H). S.L.M. acknowledges support from the National Oceanic and Atmospheric (US Department of Commerce) Grant NAOSOAR4320752. This work used eddy-covariance data acquired by the FLUXNET community and in particular by the following networks: AmeriFlux (US Department of Energy, Biological and Environmental Research, Terrestrial Carbon Program (DE-FG02-04ER63917 and DE-FG02-04ER63911)), CarboEuropeIP, Fluxnet-Canada (supported by CFCAS, NSERC, BIOCAP, Environment Canada, and NRCan), and LBA. We acknowledge the financial support to the eddy-covariance data harmonization provided by CarboEuropeIP, FAO-GTOS-TCO, iLEAPS, Max Planck Institute for Biogeochemistry, National Science Foundation, University of Tuscia, Université Laval, Environment Canada and US Department of Energy and the database development and technical support from Berkeley Water Center, Lawrence Berkeley National Laboratory, Microsoft Research eScience, Oak Ridge National Laboratory, University of California—Berkeley and the University of Virginia. This is publication 1605 of the Purdue Climate Change Research Center.

Author contributions

N.G.S., S.L.M., E.S. and J.S.D. designed the study. N.G.S. and S.L.M. performed the model simulations and analyses. All authors contributed to the interpretation of the results and writing of the manuscript.

Additional information

Supplementary information is available in the online version of the paper. Reprints and permissions information is available online at www.nature.com/reprints. Correspondence and requests for materials should be addressed to N.G.S.

Competing financial interests

The authors declare no competing financial interests.

Methods

Acclimation functions. The maximum rate of Rubisco carboxylation (V_{cmax}) and maximum rate of ribulose-1,5-bisphosphate regeneration (J_{max}) were calculated as a function of temperature[27]:

$$f(T_k) = k_{25} \exp\left[\frac{H_a(T_l - 298.15)}{298.15RT_k}\right] \frac{1+\exp\left(\frac{298.15\Delta S - H_d}{298.15R}\right)}{1+\exp\left(\frac{T_k\Delta S - H_d}{T_k R}\right)} \quad (1)$$

where k_{25} is the rate of J_{max} or V_{cmax} at 25 °C, H_a is the increase in the response below the temperature optimum, T_k is the leaf temperature in Kelvin, R is the universal gas constant (8.314 J mol^{-1} K^{-1}), H_d is the rate of decrease above the optimum, and ΔS is an entropy term related to the temperature optimum (T_{opt}) in that:

$$\Delta S = \frac{H_d}{T_{opt}} + R\ln\left[\frac{H_a}{H_d - H_a}\right] \quad (2)$$

where T_{opt} describes the optimum temperature for J_{max} or V_{cmax} (ref. 27). To simulate photosynthetic acclimation, ΔS and the ratio of J_{max} to V_{cmax} at 25 °C (J/V) were allowed to shift linearly with the 30-day acclimated temperature (T_{a30}), which was defined as the mean temperature over the previous 30 days, following Kattge and Knorr[5], such that

$$x_i = a_i + b_i \times T_{a30} \quad (3)$$

where x_i is J/V or ΔS and a_i and b_i are the intercept and slope, respectively, of the relationship between the parameter and T_{a30}. Parameterization of the model used the mean (that is, not PFT-specific) values defined in Kattge and Knorr[5]. Mean ΔS and J/V values from Kattge and Knorr[5] were used in the non-acclimated simulations.

Autotrophic dark respiration (R_d) was simulated as a function of temperature following a modified temperature-dependent Q_{10} formulation[3]:

$$R_d = R_{25} \exp\left(-\frac{T - T_{25}}{10}\right)\left(\frac{(3.22 - 0.046T)^{(3.22-0.046T)/-0.046*10}}{(3.22 - 0.046T_{25})^{(3.22-0.046T_{25})/-0.046*10}}\right) \quad (4)$$

where T is the canopy air temperature (°C) and R_{25} is the rate of respiration at 25 °C (T_{25}). Temperature acclimation of R_d was simulated using a correction factor described by Atkin *et al.*[6]:

$$R_a = R_d 10^{-0.00794(T_{a10}-25)} \quad (5)$$

where R_a is the rate of autotrophic dark respiration acclimated to the average temperature over the previous 10 days (T_{a10}; ref. 6). In non-acclimation simulations, this correction factor was not included. In all simulations $V_{cmax,25}$ was given a static PFT-specific value (see ref. 18) and R_{25} was simulated as 1.5% of $V_{cmax,25}$ following ref. 29.

Observational data. Observational site data were obtained from the FLUXNET LaThuile data set. Daily values for net ecosystem exchange (NEE) were used for comparison to model simulations. Daily values were generated using gap-filled half-hourly data. Gap filling was done following standardized protocols[30–33]. Daily data were omitted from the final analysis if less than 75% of the half-hourly data from that day were either not original or were gap-filled with low confidence. In addition, data were omitted if gross primary productivity (GPP) was less than or equal to 0. Data availability differed among sites and, as such, comparisons were made across differing time periods (see Supplementary Table 1). Information for each of the sites can be found in Supplementary Table 1 and the location of each site is plotted in Supplementary Fig. 1.

Site-level LM3 simulations. For both the model–observation comparisons and land carbon analysis simulations, simulations were performed using a modified version of the terrestrial component of the National Oceanic and Atmospheric Administration/Geophysical Fluid Dynamics Laboratory (NOAA/GFDL) Earth System Models (ESMs), Land Model version 3 (LM3; ref. 18), using the parameterizations above. Each site-level LM3 simulation was run at a single 1° grid cell encompassing one of 15 flux tower sites (see Supplementary Table 1). Locations were chosen near sites where the forest type was relatively consistent (that is, either primarily composed of broadleaf deciduous trees ($n=5$), needleleaf evergreen trees ($n=5$), or broadleaf evergreen trees ($n=5$)). As such, the plant type used in the model was set to correspond to the forest type and was not allowed to change throughout the duration of the simulation. Note that the soil respiration formulation was unchanged from the original version of LM3 (ref. 18) and not allowed to acclimate in any simulation.

For the model–observation comparisons, the model was run for 59 years (1948–2006) following a 247-year spin up, using three-hourly meteorological forcing data based on reanalysis and corrected with observations[19]. The spin up used the first 30 years (1948–1978) of the reanalysis data continuously looped for forcing. For the land carbon analysis simulations, the model was run for 239 years (1861–2100) following a 159-year spin up, forced using output from a general circulation model (GCM) simulation under the Coupled Model Intercomparison Project, phase 5 (CMIP5) representative concentration pathway (RCP) 8.5 scenario[22]. The spin up used the first 30 years of the GCM output (1861–1891) continuously looped for forcing. At each site and in both simulation types, four simulations were run: no acclimation; V_{cmax}, J_{max} and J/V acclimation (photosynthetic acclimation); R_d acclimation (respiratory acclimation); and V_{cmax}, J_{max}, J/V and R_d acclimation (full acclimation).

Following model–observation simulations, modelled daily rates of NEE were then compared to daily flux tower rates at each site using Taylor scores[20]. Taylor scores were defined as:

$$T_s = \frac{4(1+r)}{\left(\frac{s_m}{s_o} + \frac{s_o}{s_m}\right)^2 (1+r_0)} \quad (6)$$

where s is the modelled (s_m) and observed (s_o) standard deviation and r_0 is the highest possible correlation (1 in this case; ref. 20). Following future simulations, the total carbon on land during past (1890–1899), present (1990–1999) and future (2090–2099) time periods was calculated for each simulation (see Supplementary Methods).

We analysed all site-level LM3 data using a Bayesian parameter estimation approach[21]. We first calculated the difference in Taylor scores for NEE and land carbon (past, present and future) between the non-acclimation and each of the acclimation simulations at each site. We then estimated a posterior distribution for the differences in scores across all sites and within each of the three forest types, using 100,000 Markov chain Monte Carlo simulations in each case (1,000 were discarded for burn in). Improvement as a result of acclimation was assessed by examining the percentage of the posterior distribution that was greater than zero (termed PDI) as well as the range of the 95% highest density interval (HDI). If the 95% HDI did not overlap zero, acclimation was considered to have a 'significant' influence. All analyses were performed using R version 3.0.2.

Global LM3 simulations. Two global simulations were performed with the LM3 model: one with no temperature acclimation and another one with photosynthetic and respiratory temperature acclimation similar to the site-level experiments. Both LM3 simulations were driven with the forcing recorded from historical and RCP8.5 future experiments with a version of the GFDL ESM2M model. For historical period we used the observed atmospheric CO_2 concentration and for the future simulations we used the RCP 8.5 scenario values. Both experiments were spun-up for 460 years before 1860 using a fraction of historical period forcing and pre-industrial CO_2 concentration of 286 ppm. To account for acclimation effect in the LM3 simulations without retuning the rest of the model, the ratios of unacclimated to acclimated rates of V_{cmax}, J_{max} and R_d were calculated at each 30-min time step. As in the site-level simulations, R_d acclimation was applied only on leaves and only during night.

Effect of acclimation. The effect of acclimation (E_x) for each process (that is, E_v, E_j and E_r for V_{cmax}, J_{max} and R_d, respectively) was calculated as the ratio of the rate of the acclimated process to the rate of the unacclimated process. These ratios were computed at the global scale from 1861 to 2100 using high-temporal-resolution ecological and climatological Earth system model (ESM) output under historical and RCP 8.5 forcing scenario[22] simulations from the CMIP5 archive[9]. Following high-frequency computation, ratios were averaged in time, or in space and time, using one of two weighting schemes: by excluding points with zero leaf area index (LAI) and using a weighting temperature function that decreased the effect under low and high temperatures following:

$$f(T) = \frac{k_T}{(1+\exp(0.4(5-T)))(1+\exp(0.4(T-45)))} \quad (7)$$

where k_T is the rate at temperature (T) and T is the temperature in degrees Celsius; or by using monthly mean GPP or plant respiration to linearly weight V_{cmax} and J_{max} or R_d, respectively. Weights were applied to both acclimated and unacclimated rates. LAI, GPP and plant respiration values were taken from the same ESM output. The first weighting scheme allowed us to evaluate the regional patterns of acclimation (that is, Fig. 3) and avoid applying weight to time periods of no LAI or extremely low or high temperatures at which acclimation would have a small effect because of dampened physiological performance. The second scheme allowed for a better global comparison (see Fig. 2) and applied the most weight to grid cells and time points where acclimation would have the largest effect because of high flux rates. Regional calculations using the first weighting scheme were computed using ESM output from the NOAA/GFDL ESM2Mb. Global calculations using the second weighting scheme were computed using high-frequency (three-hourly)

output from three ESMs separately: NOAA/GFDL ESM2Mb, Institut Pierre Simon Laplace (IPSL) CM5A-LR and Met Office Hadley Center (MOHC) HadGEM2-ES. The MOHC HadGEM2-ES calculations were done only for three time periods for which data were available: 1960–2005, 2026–2045, 2081–2099. The high-frequency data were used to capture nonlinearities of the acclimation effect owing to the diurnal cycle of temperature.

References

29. Collatz, G. J., Ball, J. T., Grivet, C. & Berry, J. A. Physiological and environmental regulation of stomatal conductance, photosynthesis, and transpiration—a model that includes a laminar boundary layer. *Agric. For. Meteorol.* **54,** 107–136 (1991).
30. Moffat, A. M. *et al.* Comprehensive comparison of gap-filling techniques for eddy covariance net carbon fluxes. *Agric. For. Meteorol.* **147,** 209–232 (2007).
31. Papale, D. *et al.* Towards a standardized processing of Net Ecosystem Exchange measured with eddy covariance technique: algorithms and uncertainty estimation. *Biogeosciences* **3,** 571–583 (2006).
32. Papale, D. & Valentini, R. A new assessment of European forests carbon exchanges by eddy fluxes and artificial neural network spatialization. *Glob. Change Biol.* **9,** 525–535 (2003).
33. Reichstein, M. *et al.* On the separation of net ecosystem exchange into assimilation and ecosystem respiration: review and improved algorithm. *Glob. Change Biol.* **11,** 1424–1439 (2005).